Ms#2232 - APPENDIX

We have calculated, approximately, the conditions under which High Pressure Clinoenstatite/Pigeonite is predicted to exsolve from Diopside/Augite, yielding lamellae approximately parallel to (401) of the host. The experimental data needed for exact calculations are not complete. Therefore, we have employed the following rationale and procedure:

1. We have used the methodology and reasoning of Robinson et al. (1977).
2. Using the low-pressure data that are essentially complete, we established that there are no conditions under which HTclen/pig can exsolve from diopside/augite with lamellae of orientation anywhere close to (401).
3. Using the room-temperature (RT) data for pure Mg_2SiO_6 (Shinmei et al., 1999) and $CaMgSi_2O_6$ (Tribaudino et al., 2000), we determined that there are *no real solutions* of the equations of Robinson et al. (1977) for which "perfect" lamellae of pure HPclen could be exsolved from pure diopside.
4. To better understand the geometrical reasons for the result in (3), we calculated the range of values for which **a**, **c**, and β are individually consistent with lamellae of ~(401) orientation as a function of pressure. We found that the maximum and minimum values of **a** (Fig. A1) and β (Fig, A2) of host and daughter are readily compatible for formation of lamellae of the observed orientation but that the **c** parameters of HPclen are in all cases too small to yield solutions for lamellae of that orientation (Fig. A3).
5. We then considered the effect of Ca on the lattice parameters of both host and lamellae. The lamellae in this study are Ca-bearing and the host compositions are Ca-deficient compared to diopside. Addition of Ca to lamellar compositions increases the **c** parameter and reduction of Ca in host compositions decreases the **c** parameter, both of which move the system closer to compatibility with exsolution on planes approximating (401) (Fig. A3).
6. Considering further the effect of Fe in expansion of the **c** parameter of lamellae and reduction of the **c** parameter of augite, we found compatibility of ~(401) lamellae for Dabie compositions at ~9.5 GPa (Fig. A3). In order to achieve this compatibility, the effect of Fe substitution for Mg was considered to be equivalent to that of Ca substitution for Mg, which almost certainly overestimates the dilation effect of Fe. As a consequence, 9.5 GPa is a conservative estimate.
7. Applying the same methodology appropriate for the host and lamella compositions for Alpe Arami pyroxenes, we find no solution within the pressure range of experimental data (Fig. A4). Extrapolation suggests that the minimum exsolution pressure for Alpe Arami clinoenstatite is in excess of 12.5 GPa.
8. To this point, we have not considered the effect of T on lattice parameters of either hosts or lamellae because there are no data on the lattice parameters of diopside/augite at simultaneous high P and high T. To evaluate the approximate effect of T at high P, we used the lattice-parameter data of Shinmei et al. (1999) at their published high-T, high-P points and, for comparison with host pyroxenes, we applied the room-pressure thermal expansion data for diopside (Tribaudino et al., 2000) to the room-temperature lattice constants at appropriate pressures. As shown in Figs. A5-9, the data suggest that T has minimal effect, leaving our estimates of minimum pressures for exsolution of lamellae approximately parallel to (401) to be 9.5 GPa for Dabie and 12.5 GPa for Arami. Better

estimation of the conditions of exsolution will be available when the data for HPclen are extended to higher pressures and appropriate Ca contents and when diopside lattice parameters are determined at simultaneously high P and T and Ca-deficient compositions.

Methods

Robinson et al. 1977, considered two monoclinic phases, for example augite(AUG) and pigeonite(PIG), which have identical **b**-dimensions, similar crystal structure, and are intergrown so that their (010) planes are parallel. An exact phase boundary between the two intergrown phases is a plane oriented parallel to the common **b**-direction and which contains a special vector **Y** directed parallel to the common (010) plane. The magnitude of the unit-repeat of vector **Y** in terms of the augite and pigeonite unit-cell parameters is given by

(1) $|\mathbf{Y}|_{AUG} = (a^2_{AUG}x^2_{AUG} + c^2_{AUG}z^2_{AUG} + 2a_{AUG}c_{AUG}\cos\beta_{AUG}x_{AUG}z_{AUG})^{1/2}$

and

(2) $|\mathbf{Y}|_{PIG} = (a^2_{PIG}x^2_{PIG} + c^2_{PIG}z^2_{PIG} + 2a_{PIG}c_{PIG}\cos\beta_{PIG}x_{PIG}z_{PIG})^{1/2}$

where x and z are coordinates of the vector Y in the a and c directions, respectively, and a, c, and β are the unit-cell parameters at the temperature of initial phase separation. To provide an "exact lattice match" (coherence) at the phase boundary, the coincident vectors $\mathbf{Y}_{AUG}$ and $\mathbf{Y}_{PIG}$ must be equal in magnitude, thus

(3) $|\mathbf{Y}|_{AUG} = |\mathbf{Y}|_{PIG}$

In addition, there must be structural continuity across the phase boundary, which implies that there be an optimal match of the two crystal structures in the boundary region. This "best structure match" , which gives a minimum energy of atomic misfit at the boundary, is obtained when the x and z coordinates of the vectors $\mathbf{Y}_{AUG}$ and $\mathbf{Y}_{PIG}$ are equal; thus

(4) $x_{AUG} = x_{PIG}$ and $z_{AUG} = z_{PIG}$

Equating (1) and (2) and setting z = 1

(5) $(a^2_{AUG} - a^2_{PIG})\,x^2 + (2a_{AUG}c_{AUG}\cos\beta_{AUG} - 2a_{PIG}c_{PIG}\cos\beta_{PIG})\,x + (c^2_{AUG} - c^2_{PIG}) = 0$

which is of the form

(6) $A\,x^2 + B\,x + C = 0$

Solving for the two real values of x gives the two possible orientations ("001" and "100") of the exact phase boundary

(7) $x = [-B \pm (B^2 - 4AC)^{1/2}]/2A$

The intercepts of the two possible boundary planes with the a, b, and c axes are thus x_1, y = ∞, z = 1 and x_2, y = ∞, z = 1. If x <-1 or x > 1, the phase boundary is defined as having an "001" orientation. If -1 < x <1 the phase boundary is defined as having a "100" orientation.

The orientation of the phase boundary, as defined by the acute angle formed between the vector Y and the a or c axis of a particular phase, is given by

(8) $a_i \wedge \mathbf{Y} = \pm\sin^{-1}(c_i\sin\beta_i/|\mathbf{Y}|)$

and

(9) $c_i \wedge \mathbf{Y} = \pm\sin^{-1}(a_i\sin\beta_i|x|/|\mathbf{Y}|)$

where

(10) $|\mathbf{Y}| = [(a_i x)^2 + c_i^2 + 2a_i c_i x\cos\beta_i]^{1/2}$

and a_i, c_i, and β_i refer to the unit-cell parameters of augite or pigeonite.

If x > 0, the vector **Y** is directed toward the obtuse β angle of augite or pigeonite (between the $+a$ and $+c$) and the angles $a_i \wedge \mathbf{Y}$ and $c_i \wedge \mathbf{Y}$ given by (8) and (9) are defined as negative. If x < 0,

the vector **Y** is directed toward the acute β angle of augite or pigeonite (between the -a and +c) and the angles $a_i \wedge \mathbf{Y}$ and $c_i \wedge \mathbf{Y}$ given by (8) and (9) are defined as positive.

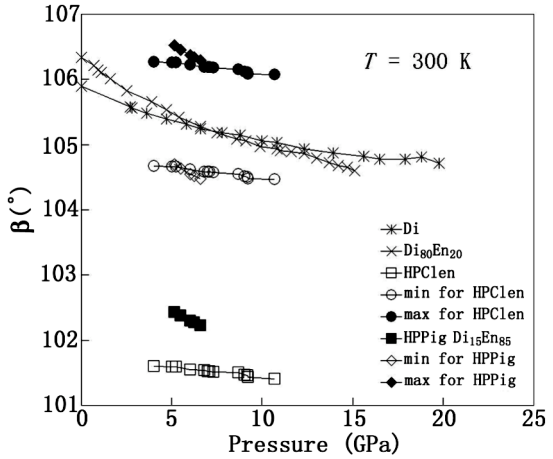

Figure A1. β parameters of Di, Di80En20, HPClen and HPPig (Tribaudino et al. 2000, Shinmei et al.1999, Nestola et al.2004), and the calculated possible β parameters of Di (or Aug) for yielding //(401) HPClen and HPPig exsolutions.

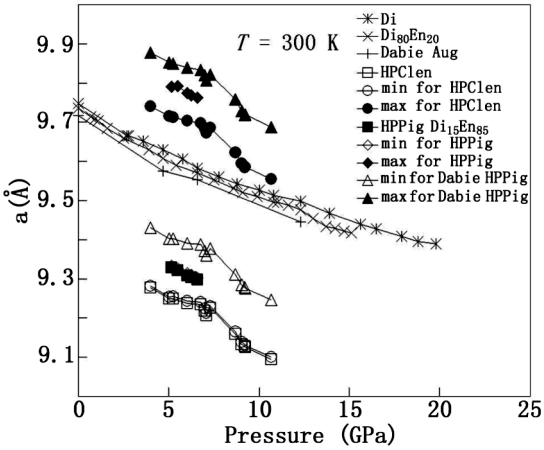

Figure A2. *a* parameters of Di, $Di_{80}En_{20}$, HPClen and HPPig (Tribaudino et al. 2000, Shinmei et al.1999, Nestola et al.2004), and the calculated possible *a* parameters of Di (or Aug) for yielding //(401) HPClen and HPPig exsolutions, and the estimated band for Dabie HPPig. The *c* parameters of Dabie Aug estimated according to Di and $Di_{80}En_{20}$.

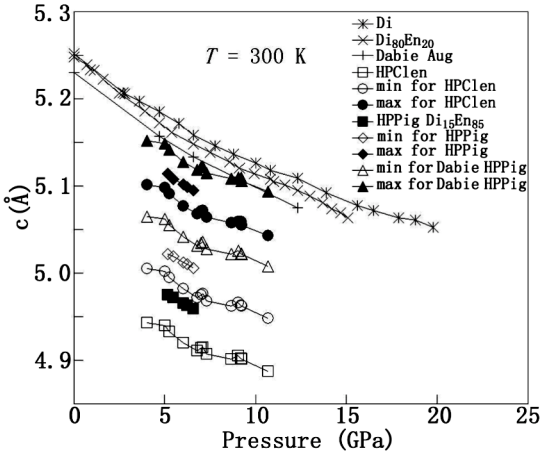

Figure A3. *c* parameters of Di, $Di_{80}En_{20}$, HPClen and HPPig(Tribaudino et al. 2000, Shinmei et al.1999, Nestola et al.2004), and the calculated possible *c* parameters of Di (or Aug) for yielding //(401) HPClen and HPPig exsolutions, and the estimated band for Dabie HPPig. The *c* parameters of Dabie Aug estimated according to Di and $Di_{80}En_{20}$.

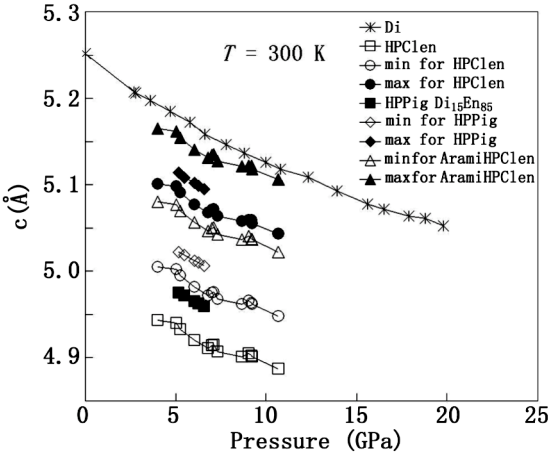

Figure A4. *c* parameters of Di, HPClen and HPPig (Tribaudino et al. 2000, Shinmei et al.1999, Nestola et al.2004), and the calculated possible *c* parameters of Di (or Aug) for yielding //(401) HPClen and HPPig exsolutions, and the estimated band for Arami HPClen.

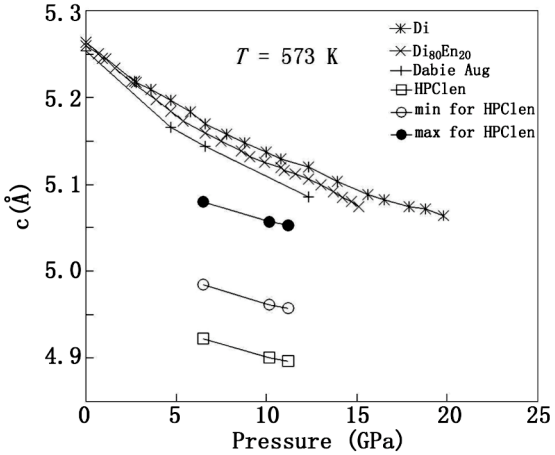

Figure A5. *c* parameters of Di, $Di_{80}En_{20}$, HPClen (Tribaudino et al. 2000, Shinmei et al.1999), and the calculated possible *c* parameters of Di (or Aug) for yielding //(401) HPClen exsolutions under *T*=573K. The *c* parameters of Dabie Aug estimated according to Di and $Di_{80}En_{20}$.

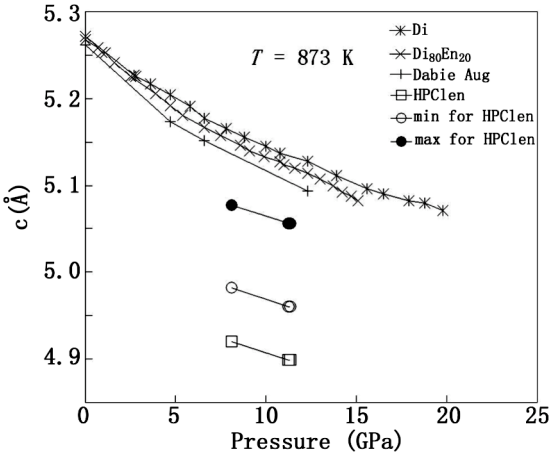

Figure A6. *c* parameters of Di, $Di_{80}En_{20}$, HPClen (Tribaudino et al. 2000, Shinmei et al.1999), and the calculated possible *c* parameters of Di (or Aug) for yielding //(401) HPClen exsolutions under *T*=873K. The *c* parameters of Dabie Aug estimated according to Di and $Di_{80}En_{20}$.

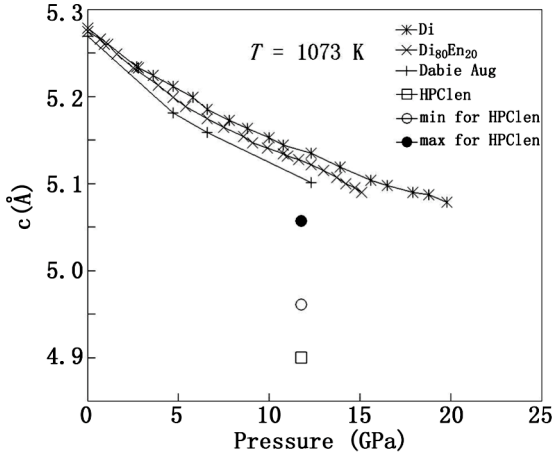

Figure A7. *c* parameters of Di, $Di_{80}En_{20}$, HPClen (Tribaudino et al. 2000, Shinmei et al.1999), and the calculated possible *c* parameters of Di (or Aug) for yielding //(401) HPClen exsolutions under *T*=1073K. The *c* parameters of Dabie Aug estimated according to Di and $Di_{80}En_{20}$.

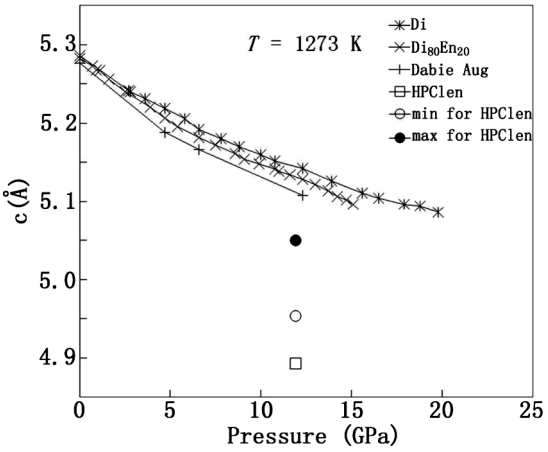

Figure A8. *c* parameters of Di, $Di_{80}En_{20}$, HPClen (Tribaudino et al. 2000, Shinmei et al.1999), and the calculated possible *c* parameters of Di (or Aug) for yielding //(401) HPClen exsolutions under *T*=1273K. The *c* parameters of Dabie Aug estimated according to Di and $Di_{80}En_{20}$.

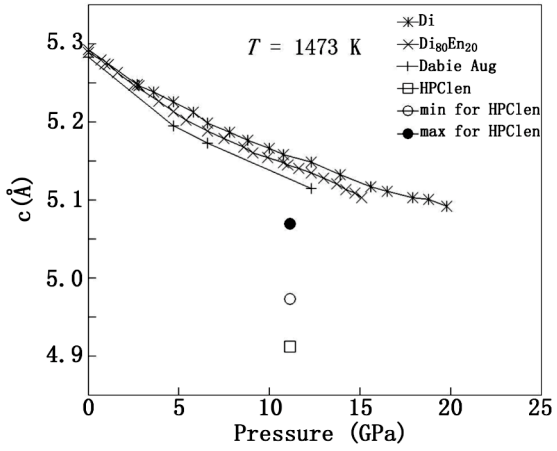

Figure A9. *c* parameters of Di, $Di_{80}En_{20}$, HPClen (Tribaudino et al. 2000, Shinmei et al.1999), and the calculated possible *c* parameters of Di (or Aug) for yielding //(401) HPClen exsolutions under *T*=1473K. The *c* parameters of Dabie Aug estimated according to Di and $Di_{80}En_{20}$.